IOP Conference Series: Earth and Environmental Science

Soil carbon and nitrogen stocks in polygonal-fissure mires of southern tundra in Western Siberia

To cite this article: L L Golubyatnikov and E A Zarov 2022 *IOP Conf. Ser.: Earth Environ. Sci.* **1093** 012024

View the article online for updates and enhancements.

Soil carbon and nitrogen stocks in polygonal-fissure mires of southern tundra in Western Siberia

L L Golubyatnikov[1*] and E A Zarov[2]

[1]Laboratory of Mathematical Ecology, A.M. Obukhov Institute of Atmospheric Physics, Russian Academy of Sciences, 3, Pyzhevsky Lane, Moscow, 119017, Russian Federation
[2]Research Education Center of Environmental Dynamics and Climate Change, Yugra State University, 16, Chekhov st., Khanty-Mansiysk, 628012, Russian Federation

*E-mail: golub@ifaran.ru

Abstract. Based on the experimental data, soil carbon and nitrogen stocks are estimated in polygonal–fissure mires of southern tundra in the north–eastern part of Western Siberia. The field experiments were carried out in 2014–2017 at the site located in tundra zone of the Yamal–Nenets Autonomous District. Active soil layer (seasonally thaw) and upper frozen layer are investigated. The seasonally thaw layer of tundra soils has been subdivided into two horizons: active upper layer (down to 15 cm depth) and active lower layer (from 15 cm down to the permafrost). Our research has shown that the values of organic carbon and total nitrogen storages in mires under study can be estimated as 14.1±3.6 kgC/m^2 and 0.4±0.1 kgN/m^2 for the active soil layer and 12.9±2.8 kgC/m^2 and 0.5±0.1 kgN/m^2 for the upper frozen layer. Organic carbon and total nitrogen stocks for the active soil layer and upper frozen layer in polygonal-fissure mires are evaluated as 172.0±29.1 ktC and 5.4±1.2 ktN.

1. Introduction

Current climate change is most noticeable at high latitudes [1–3]. Over the last three decades, the average annual air temperature in the north of Russia has increased by 0.8–1.3 °C, and the increasing air temperature trend is 1.2–1.5 times higher for a long cold period in this region than for a short warm one [4]. During the last decade, the permafrost warmed by 0.39 °C and 0.20 °C in the Arctic continuous and discontinuous zones respectively [5]. According to calculations with the atmosphere–ocean coupled general circulation models, significant climatic changes, primarily an increase in air temperature, are also expected in the arctic regions in the future [6–8]. Predicted climate changes may cause the permafrost degradation and an increase of the thaw layer thickness in subpolar regions. Climate warming will lead to intensification of the carbon and nitrogen fluxes between the atmosphere and tundra ecosystems. In particular, carbon and nitrogen sequestrated in the upper frozen soil layers will be involved in the active biochemical cycle due to seasonal deeper thawing. The emission of greenhouse gases (such as carbon dioxide, methane, and nitrous oxide) from tundra ecosystems to the atmosphere might be significantly increased as a result of the expected climate warming [5, 9–13].

Northern peatlands have accumulated large stocks of carbon and nitrogen, but their estimates remain variable and uncertain. Thus, the estimated amounts of carbon and nitrogen in northern peatlands range from 185 GtC to 1055 GtC and from 7 GtN to 15 GtN respectively [12, 14, 15].

Usually the estimates of the soil carbon and nitrogen pools for northern ecosystems are based on the limited number of observational data. It may lead to assessment mistakes. For this reason, an important task is to expand the carbon and nitrogen soil stock database for permafrost ecosystems in the Arctic regions.

Polygonal–fissure mires are typical peatland type of southern tundra. The mires have a complex structure of alternating elevated polygons and frost–shattered fissures separating the polygons. The thickness of peat deposits in polygons is about 1.5–2.0 m, sometimes it exceeds 3.0 m. The surface of the polygons is usually small tussocky, sometimes even. The polygons have four–, five–, six– and heptagonal shapes with a side length of 5–14 m. The width of fissures varies from 1 to 3 m. When intersecting the fissures form rather wide areas with hollows [16, 17]. The polygons are covered by lichens, sphagnum mosses, small ericaceae shrubs and dwarf birch. The fissures are occupied by hygrophilous grass–moss communities of sphagnum mosses, sedges, cotton grasses with single specimens of andromeda.

The aim of this study is to estimate carbon and nitrogen stocks in the modern active soil layer (annual summer thawing layer) and upper permafrost layer of polygonal–fissure mires for the research site in the southern tundra of Western Siberia based on field works and satellite image analysis.

2. Materials and methods

The study site is located on the Pur–Taz watershed in the southern tundra zone of Western Siberia, approximately 20 km southwest from the urban settlement Tazovsky in the Yamal–Nenets Autonomous District (figure 1). The territory under study is 40 km^2 area and it is located in the region of continuous permafrost. The climate is sharply continental with a short and cool summer, long and cold winter: the mean annual air temperature is –6.5 ºC, the growing season is about 100 days. The mean air temperature of the coldest month (January) is –25.4 °C, the mean air temperature of the warmest month (July) is +15.4 °C. The annual mean precipitation (period from 2005 to 2017) is 570 mm [16].

The microlandscapes pattern of the study site is analyzed on the basis of high-resolution satellite image (WorldView–2) and field data [16, 18]. The field work was carried out in summer seasons from 2014 to 2017. All microlandscapes of polygonal–fissure mires were visited and identified during the field expeditions [19]. For each microlandscape, the vegetation and microrelief are described and the depths of thawing layer are measured. The depths of water table, values of acidity and electrical conductivity of water are determined for the waterlogged microlandscapes [16]. Soil samples were collected in three replications from each microlandscape, and from three different soil horizons –

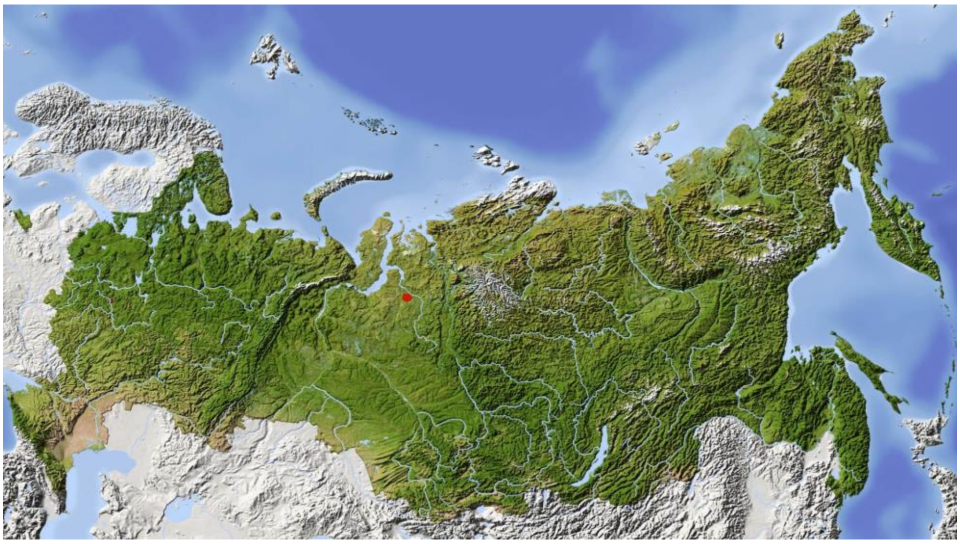

Figure 1. Research area location (red circle).

active upper layer (~0–15 cm), active lower layer (~15–35 cm) and upper frozen layer (~35–45 cm). For each microlandscape 81 soil samples were considered. For the microlandscapes under study the active upper layer consists of organic litter with high live root penetration, the active lower layer consists of peat.

The values of acidity and electrical conductivity of water were measured with a portable measuring device Hanna 98129 (Hanna Instruments, USA) during the field season. The main soil properties were determined in the laboratory. Carbon and nitrogen contents in the soil samples were determined using an elemental analyzer (EuroVector EA–3000). The elemental analyzer was calibrated by Atropine (C=70.56%, N=4.84%, H=8.01%, O=16.59%). Prior the measurements, the soil samples containing traces of carbonates were acidized. The bulk density of the soil samples was calculated using the dry mass of the samples and the volume of a cylindrical subsample.

Soil carbon and nitrogen storages were computed for each layer taken separately from carbon and nitrogen contents, layer depth, and bulk density data according to the following equation:

$$Stg = BD \times Cn \times LD \times 10^{-1} \quad (1)$$

where *Stg* is the total amount of an element (soil organic carbon or total nitrogen) for given depth ($kg \cdot m^{-2}$), *Cn* is element content for given depth (%), *BD* is dry bulk density ($g \cdot cm^{-3}$), *LD* is depth of soil layer (cm).

Soil carbon and nitrogen stocks were computed for each microlandscapes as:

$$Stk = \sum_{i=1}^{3} Stg_i \times S \times 10^{-3} \quad (2)$$

where *Stk* is the total amount of an element (soil organic carbon or total nitrogen) for given microlandscape (in ton), *S* is microlandscape area (m^2).

3. Results and discussion

The microlandscape pattern of our key site is analyzed on the basis of WorldView–2 satellite image. According to the calculation results, the polygonal–fissure mires occupy a significant part (~31%) of the wetland territory under consideration. The microlandscape pattern of the polygonal–fissure mires is formed by lichen–moss–shrub communities, lichen–shrub communities, moss–shrub communities, frost–shattered fissures, and wetland ponds [16]. The pictures of microlandscapes of the polygonal-fissure mires are illustrated in figure 2. Lichen–moss–shrub communities on polygons are found in central parts of polygonal-fissure mires. Lichens *Cladonia stellaris* and *C. stygia* form a continuous cover between tussocks. Vegetation of the tussocks is represented by mosses *Sphagnum fuscum*, *Sph. capillifolium*, lichens *Cladonia stellaris*, *C. stygia*, herb-shrub communities from *Rubus chamaemorus*, *Ledum palustre*, and small shrubs *Betula nana*. Lichen–shrub communities on polygons occupy the border zones of polygonal-fissure mires. The area between the tussocks is occupied by lichens *Cladonia stellaris*, *C. stygia* with a share of *C. rangiferina*, *C. amaurocraea*, and *Cetraria cucullata*. The shrubs are concentrated on tussocks and consist of *Ledum palustre* with single specimens of *Betula nana*. The mosses *Sphagnum fuscum*, *Sph. capillifolium* are found on tussocks with rare spots. The grass layer is represented by *Rubus chamaemorus*. Moss–shrub communities on polygons are found on the margins of polygons, which are prone to water–thermal erosion. The moss cover consists mainly of *Sphagnum fuscum* with *Sph. balticum*, *Sph. lenense*. Lichens *Cladonia stellaris* and *C. stygia* are distributed in sparse spots. The grass layer is formed by *Rubus chamaemorus*. The sparse shrubs are represented by *Andromeda polifolia*, *Ledum palustre*, *Betula nana*. Ponds occupy the central part of some poligons. There is a water depression caused by local thermokarst processes. Frost–shattered fissures between polygons are small trenches (1–3 m wide) formed as a result of frost cracking. The mosses *Sphagnum balticum*, *Sph. lindbergii*, *Sph. jensenii*, *Sph. majus* form a continuous cover. The grass layer is represented by *Carex rotundata* and *Eriophorum russeolum*. Dwarf shrubs *Betula nana* and *Andromeda polifolia* are rare.

The measured values of the acidity and electrical conductivity of the mire water, thawing layer depth and water table depth for each microlandscape under study are presented in table 1. The minimum thawing layer depth of peat deposits in polygonal–fissure mires is found in microlandscapes with moss and shrub communities (25–28 cm). The thawing layer of fissures separating the polygons is largest (31–45 cm). The water table depths in the microlandscapes of the mires is observed from 3 down to 22 cm. The peat deposits under lichen–moss–shrub and lichen–shrub communities on polygons have no the water table. The bog waters in the polygonal–fissure mires of the studied region have pH from 3.2 to 4.7 and electrical conductivity from 8 to 64 μS/cm.

The soil bulk density is a reliable indicator of the mineral or organic nature of a soil [15]. According to our research, the bulk density for seasonally thawed layer in the studied microlandscapes ranges from 0.034 to 0.202 $g \cdot cm^{-3}$, with a mean value of 0.124±0.087 $g \cdot cm^{-3}$ (mean±standard deviation) and a median of 0.126 $g \cdot cm^{-3}$. The bulk density values for upper permafrost layer ranges from 0.222 to 0.356 $g \cdot cm^{-3}$, with a mean value of 0.301±0.064 $g \cdot cm^{-3}$ and a median of 0.312 $g \cdot cm^{-3}$. The obtained bulk density values correspond to organic rich soil [15, 20].

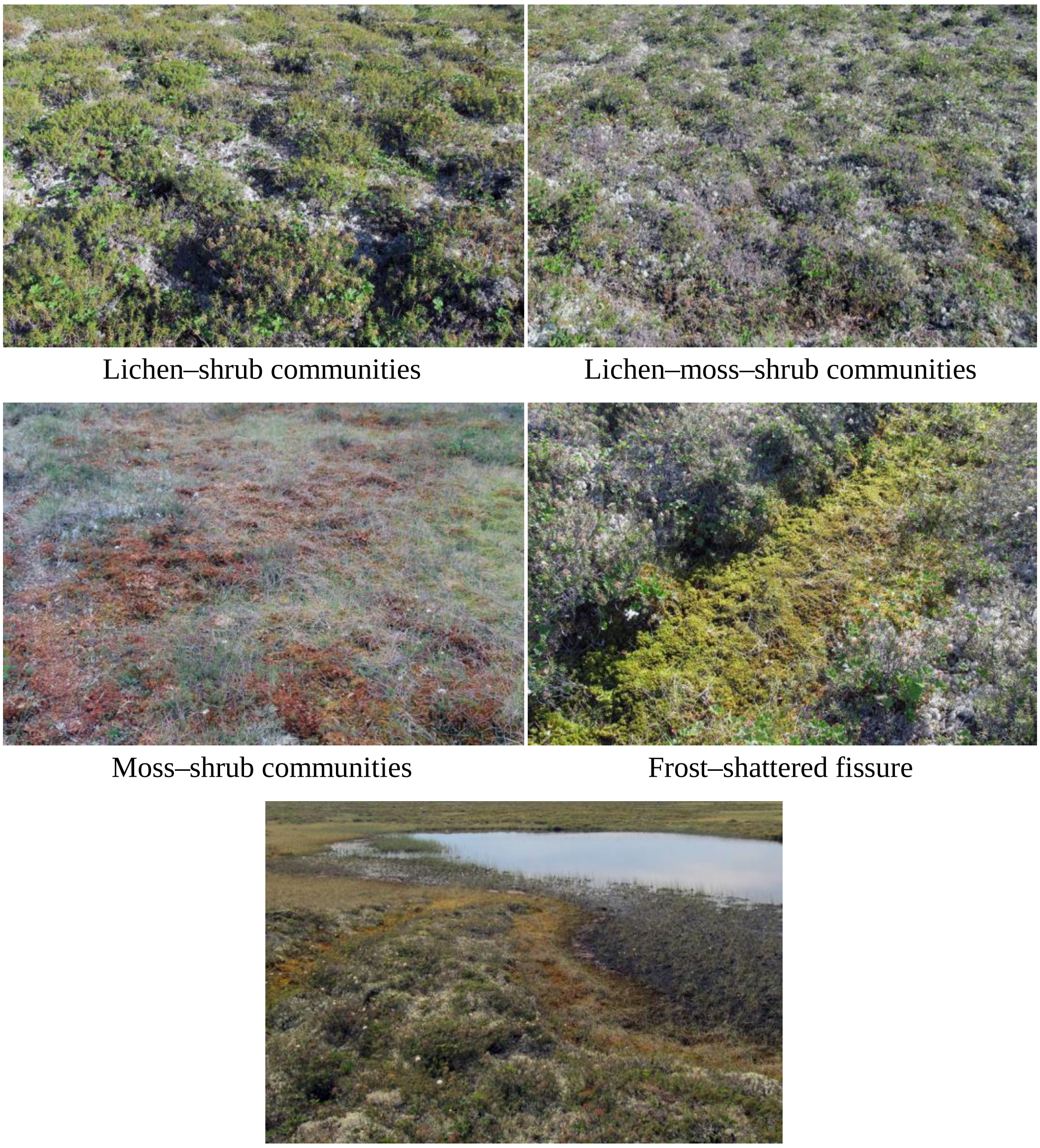

Lichen–shrub communities Lichen–moss–shrub communities

Moss–shrub communities Frost–shattered fissure

Wetland pond

Figure 2. Microlandscapes of polygonal-fissure mires.

Organic carbon and total nitrogen contents in the researched soil layers of microlandscapes of the polygonal-fissure mires are shown in figure 3. The obtained results show the similar carbon content in seasonally thaw and upper frozen layers of microlandscapes under study. The active upper layer has 43–49% of carbon, the active lower layer – 42–50%, the upper frozen layer – 44–50%. The differences of carbon content inside a thaw layer between the active upper zone and the active lower zone are 2–4%. It should be noted that the carbon content in the peat layers of polygon mires is characterized by variability. According to our results, the total nitrogen content increase from the active upper layer to the upper frozen layer (with the exception of active lower layer in frost–shattered fissures). The lowest nitrogen content is found in the active lower layer of moss–shrub communities

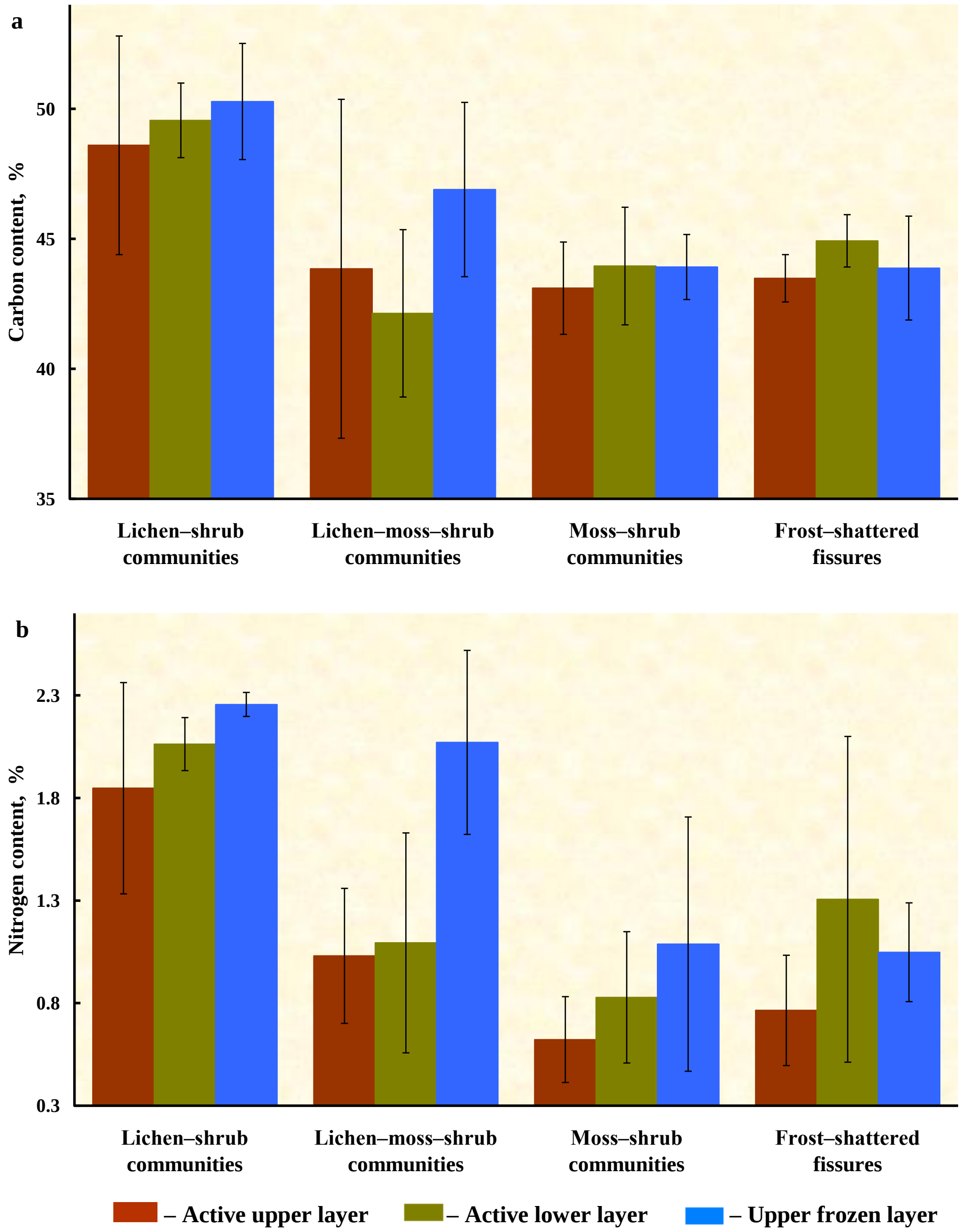

Figure 3. Estimates of organic carbon (a) and total nitrogen (b) contents in soil layers of microlandscapes for polygonal-fissure mires (average values and standard deviations).

on polygons (0.6%), the highest nitrogen content is found in the upper frozen layer of lichen–shrub communities on polygons (2.3%).

Organic carbon and total nitrogen storages in the studied soil layers of microlandscapes for polygonal-fissure mires are presented in figure 4. According to our calculations as per formula (1), the values of organic carbon and total nitrogen storage in the thawing soil layer vary from 5.3 to 23.1 kgC/m^2 and from 0.1 to 0.9 kgN/m^2 depending on the microlandscape type. The upper frozen soil horizon contains 9.8–23.9 kg/m^2 of organic carbon and 0.2–1.1 kg/m^2 of nitrogen. Organic carbon and total nitrogen storages in the soils of the polygons (Lena River Delta) published by Zubrzycki *et al*. [21] within 30 cm depth were 7.5–8.8 kgC/m^2 and 0.06–0.76 kgN/m^2 respectively. Our results for the

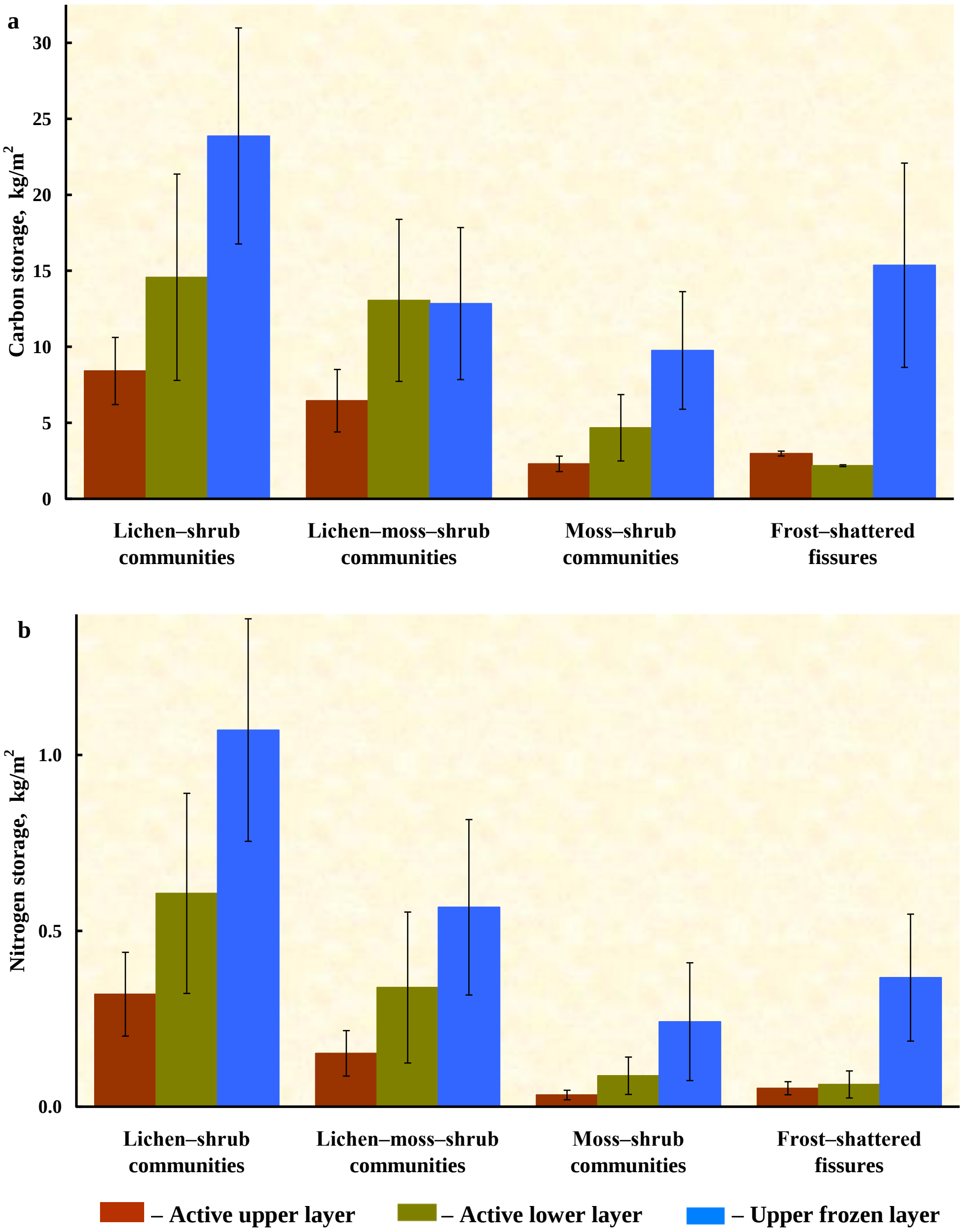

Figure 4. Estimates of organic carbon (a) and total nitrogen (b) storages in soil layers of microlandscapes for polygonal-fissure mires (average values and standard deviations).

Table 1. Microlandscape descriptions.

	TL[a] (cm)	WT[b] (cm)	Ph[c]	EC[d] (μS/cm)
Lichen–moss–shrub communities	28–30	–	–	–
Lichen–shrub communities	25–28	–	–	–
Moss–shrub communities	29–33	12–22	3.2–3.5	49–64
Frost–shattered fissures	31–45	3–17	3.8–4.2	21–43
Wetland ponds	–	–	3.9–4.7	8–38

[a]TL – thawing layer depth.
[b]WT – water table depth.
[c]Ph – acidity of water.
[d]EC – electrical conductivity of water.

thawing soil layer are comparable with the storage estimates of [21]. Gentsch *et al.* [22] reported carbon and nitrogen storages of 10.8–15.4 kgC/m^2 and 0.8–1.1 kgN/m^2 for the thawing layer of well-drained permafrost soil in the Siberian Arctic. The storage estimates found in our study are lower than the estimates in [22].

The values of organic carbon and total nitrogen stocks for the studied soil layers in polygonal-fissure mires are calculated using formula (2). The active upper layer of soils for mires under study contains 30.7±6.2 ktC and 0.7±0.2 ktN. The organic carbon and total nitrogen stored within the active lower soil layer are estimated at 59.1±16.7 ktC and 1.6±0.7 ktN. The upper frozen soil layer is characterized by values of carbon and nitrogen stocks at 82.2±18.0 ktC and 3.1±0.9 ktN.

4. Conclusions

The polygonal–fissure mires occupy about a one–third of the wetland territory in our key site in the southern tundra of Western Siberia. Lichen–moss–shrub communities, lichen–shrub communities, moss–shrub communities, frost–shattered fissures, and wetland ponds form the microlandscape pattern of the mires. The mean active soil layer (seasonally thaw layer) of polygonal–fissure mires was 27.1±5.3 cm (ranging from 25 to 45 cm) at the time of sampling. The bog waters have an acidic pH in the range from 3.2 to 4.7 and low values of electrical conductivity (<64 μS/cm). According to our calculation, the values of organic carbon and total nitrogen storages in mires under study can be estimated as 14.1±3.6 kgC/m^2 and 0.4±0.1 kgN/m^2 for the active soil layer and 12.9±2.8 kgC/m^2 and 0.5±0.1 kgN/m^2 for the upper frozen layer. Organic carbon and total nitrogen stocks for the active soil layer and upper frozen layer in polygonal–fissure mires are evaluated as 172.0±29.1 ktC and 5.4±1.2 ktN.

Acknowledgements

This study was supported by the Russian Foundation for Basic Researchers (Projects 14–05–00193), and State assignments FMWR-2022-0015 (1021032424681-6-1.5.10; 1.5.8; 1.6.19).

References

[1] Bindoff N L *et al* 2013 Detection and Attribution of Climate Change: from Global to Regional Climate Change 2013 *The Physical Science Basis Contribution of Working Group I to the Fifth Assessment Report of the Intergovernmental Panel on Climate Change* (Cambridge, United Kingdom and New York, NY, USA: Cambridge University Press) pp 867–952
[2] Streletskiy D A, Sherstiukov A B, Frauenfeld O W and Nelson F E 2015 *Environmental Research Letters* **10** 12500
[3] Eliseev A V 2011 *Izvestiya, Atmospheric and Oceanic Physics* **479** 131–53
[4] Pavlov A V 2008 *Cryolithozone Monitoring* (Novosibirsk: Geo) p 229
[5] Biskaborn B K *et al* 2019 *Nature Communications* **10** 264–78

[6] Collins M *et al* 2013 Long-term Climate Change: Projections Commitments and Irreversibility Climate Change 2013 *The Physical Science Basis Contribution of Working Group I to the Fifth Assessment Report of the Intergovernmental Panel on Climate Change* (Cambridge, United Kingdom and New York, NY, USA: Cambridge University Press) pp 1029–136
[7] Arzhanov M M, Eliseev A V and Mokhov I I 2012 *Global and Planetary Change* **86–87** 57–65
[8] Eliseev A V and Semenov V A 2016 *Doklady Earth Sciences* **471** 1183–7
[9] Karelin D V and Zamolodchikov D G 2008 *Carbon Exchange in Cryogenic Ecosystems* (Moscow: Nauka) p 344
[10] Golubyatnikov L L, Mokhov I I and Eliseev A V 2013 *Izvestiya Atmospheric and Oceanic Physics* **49** 229–43
[11] Voigt C *et al* 2017 *Proc. of the National Academy of Sciences* **114** 6238–43
[12] Hugelius G *et al* 2020 *Proc. of the National Academy of Sciences* **117** 20438–46
[13] Luan J *et al* 2019 *Communications Biology* **2** 132
[14] Nichols J E and Peteet D M 2019 *Nature Geoscience* **12** 917–21
[15] Loisel J *et al* 2014 *The Holocene* **24** 1028–42
[16] Zarov E A, Golubyatnikov L L, Lapshina E D and Loyko S V 2022 *Biology Bulletin* **49** 118–27
[17] Golubyatnikov L L and Zarov E A 2019 *Ecology. Economy. Informatics.: System analysis and mathematical modeling of ecological and economic systems* **4** 92–5
[18] Golubyatnikov L L *et al* 2015 *Izvestiya Atmospheric and Oceanic Physics* **51** 969–78
[19] Zarov E A, Golubyatnikov L L and Lapshina E D 2016 *Report Series in Aerosol Science* **180** 590–3
[20] Khrenov V Ya 2011 *West Siberian Soils of Cryolithozone* (Novosibirsk: Nauka) p 211
[21] Zubrzycki S *et al* 2013 *Biogeosciences* **10** 3507–24
[22] Gentsch N *et al* 2015 *Biogeosciences* **12** 4525–42